Korean J. Chem. Eng., **25**(2), 245-252 (2008)

Testing of PEM fuel cell performance by electrochemical impedance spectroscopy: Optimum condition for low relative humidification cathode

Kengkaj Pattamarat and Mali Hunsom†

Fuels Research Center, Department of Chemical Technology, Faculty of Science,
Chulalongkorn University, Bangkok 10330, Thailand
(*Received 2 November 2006 • accepted 9 July 2007*)

Abstract−Electrochemical impedance spectroscopy (EIS) was used to investigate the influence of several parameters on the performance of PEMFC. The applied frequency was in the range of 50 mHz-10 kHz. The experiment was designed by using a 2^k factorial design to identify the effects of various parameters including cell voltage, flow rates of gaseous fuels and cell temperature at the saturated humidification in anode and 60% relative humidity cathode. The results indicated that the cell temperature, cell voltage and interactions of cell voltage, flow rate of H_2 and O_2 had a significant effect on the cell performance. In addition, the flow rate of O_2 had a strong effect on the ohmic resistance and the charge transfer resistance in the system. Models describing the relationship between previous parameters and ohmic resistance, charge transfer resistance and capacitance were also developed.

Key words: Electrochemical Impedance Spectroscopy, Membrane Electrode Assembly, PEM Fuel Cell, Relative Humidification, Factorial Design

INTRODUCTION

The proton exchange membrane fuel cell (PEMFC), also called "the solid polymer fuel cell" (SPFC), was first developed by General Electric in the USA in the 1960's. It is one of the most promising candidates as a clean power source for electric vehicles or combustion engines in automotive transport, because of (i) its high energy conservation efficiency, (ii) the possibility of using regenerative fuels, (iii) low or zero noxious emission of environmental pollutant, (iv) low operating temperature, and (v) relatively quick startup [1-3]. Due to the complexity in electrode behavior inside a fuel cell and the influence of several factors, electrochemical impedance spectroscopy (EIS) has been demonstrated to be a useful and powerful technique to study the different processes taking place in fuel cells. In this technique, the cell or electrode impedance is plotted versus frequency of the AC source. The variation of the impedance with frequency is often of interest and can be displayed in different ways. In a Bode plot, log|Z| and ϕ are plotted against logarithm value of frequency (ω). An alternative representation, a Nyquist plot, displays Z_{Im} versus Z_{Re} for different values of ω The potential losses for an H_2/O_2 fuel cell may cause several steps: interfacial reactions kinetics, conductance of the electrolyte in the catalyst layer, oxygen diffusion in the gas phase, in the thin film and in the distributed agglomerate regions of the gas diffusion electrodes and the balance water in the membrane [4]. Application of EIS for testing the various processes occurring in a fuel cell can be done in many ways for various kinds of fuel cells such as solid oxide fuel cells [5-7] and direct methanol fuel cells [8-10]. Focusing on the proton exchange fuel cell, Wagner et al. [11] investigated the transportation of water in membrane by using this tool. They reported that the water transport in the membrane played an important role in establishing the limiting polarization behavior at high current density. Eikerling et al. [12] demonstrated that the catalyst layer thickness had significant effect on transportation of active species in a fuel cell. When the characteristic length scales of both transport processes (O_2 and H^+) were large compared with the catalyst layer thickness, the impedance response merely consisted of a semicircle. The proton transport limitation was observed as a straight line in the high frequency domain, and the impedance response was corresponding to the equivalent circuit of a linear ladder network composed of the proton resistances and capacitances. By changing the cell voltage of mono cathode cell [13], the charge transfer resistance decreased exponentially during the whole range of potential explored (0.5-0.9 V). The formation of cathode capacitance was achieved after polarization of about 200 mV from open circuit potential (0.5 V), and it was kept constant (4.6 mF) for larger currents due to faster double layer discharge. In addition, the limiting capacitance was a function of mass of catalyst in fuel cell [14]. According to the effect of membrane thickness, the cells with thinner membranes exhibited less sensitivity to a change in temperature and current density [15]. Increasing membrane thickness led to a shorter relaxation time. If membranes with high equivalent weight (EW) were employed, the value of the total charge transfer resistance increased almost doubly due to the water shortage for proton hydration [16]. In an H_2/air fuel cell, the impedance spectra of the air cathode was shown to contain two features [17,18]: a high frequency loop (HF) and a low frequency loop (LF). The HF loop was responsible for the process occurring in the cathode catalyst layer: interface charge transfer and mass transport of air in the pores of the catalyst layer (agglomerate diffusion) and in the thin Nafion layer surrounding catalyst particles (thin film diffusion). In the presence of CO at anode side, the EIS spectra exhibited the pseudo-inductive contributions at the low frequency part due to a surface relaxation [19,20]. On the other hand, in the presence of NO_x, the impedance spectra indicated that NO_x can cause a significant decay of the fuel cell performance, but the cell perfor-

†To whom correspondence should be addressed.
E-mail: mali.h@chula.ac.th

Table 1. Response of 2^4 factorial design

Run no.	A	B	C	D	R_{Ω} (Ω)		R_{ct} (Ω)		C_d (μF)	
					Rep. 1	Rep. 2	Rep. 1	Rep. 2	Rep. 1	Rep. 2
1	-	-	-	-	0.1312	0.1625	0.2299	0.3219	45560	37963
a	+	-	-	-	0.2349	0.2856	0.4514	0.5682	19884	25091
b	-	+	-	-	0.2415	0.2249	0.4328	0.4449	28232	27467
ab	+	+	-	-	0.2483	0.2689	0.4268	0.5858	24534	24340
c	-	-	+	-	1.1972	1.2957	3.7217	3.4086	5099	4887
ac	+	-	+	-	1.4392	1.2222	3.8128	3.1933	6253	5217
bc	-	+	+	-	0.9344	1.2101	2.5551	3.8061	6520	4377
abc	+	+	+	-	0.2653	0.2419	0.8064	0.7789	17680	11523
d	-	-	-	+	0.1675	0.2100	4.1874	4.1463	74920	47597
ad	+	-	-	+	0.1721	0.2095	4.4493	3.7783	70510	44755
bd	-	+	-	+	0.1348	0.1307	2.2517	1.6415	75099	47576
abd	+	+	-	+	0.1638	0.2071	3.9620	3.2748	79182	44243
cd	-	-	+	+	0.9409	1.0843	12.3465	12.4322	8616	6282
acd	+	-	+	+	0.1859	0.2487	3.6974	3.7881	39186	32773
bcd	-	+	+	+	0.2869	0.2903	5.8844	4.6895	18078	30896
abcd	+	+	+	+	1.3620	1.1279	17.7091	16.4928	8182	11966
Axial	−1.414	0	0	0	0.6341	0.5542	5.9588	5.3227	9622	9230
Axial	1.414	0	0	0	0.5878	0.5845	4.2667	3.8451	9866	10948
Axial	0	−1.414	0	0	0.6390	0.6261	5.5837	4.0439	8799	8920
Axial	0	1.414	0	0	0.5493	0.5762	4.3309	4.8771	7136	8631
Axial	0	0	0	−1.414	0.5434	0.6208	1.9860	1.9168	7179	7438
Axial	0	0	0	1.414	0.4707	0.4768				
Center	0	0	0	0	0.5646		3.1561		11429	
Center	0	0	0	0	0.5493		3.2378		11140	
Center	0	0	0	0	0.6125		3.7927		11099	

mance could be recovered after the introduction of NO_x was discontinued [21].

In this work, the influence of several parameters on the performance of the low humidification PEM fuel cell was explored by using EIS together with the 2^k factorial design.

EXPERIMENT

The optimum working condition of an H_2/O_2 fuel cell was investigated by using EIS. A commercial single cell from ElectroChem, Inc., USA (FC05-01SP) having an active surface area of 5 cm^2 (Pt loading 1 mg/cm^2) was employed in this study. The impedance data were recorded in the frequency range from 50 mHz-10 kHz with applied AC amplitude of 20 mV. A potentiostate (Autolab, PGSTAT30) and a frequency response analyzer (FRA) interfaced with a computer were used to analyze the performance of the single fuel cell. The experiment was carried out with the saturated relative humidity of gas fed to anode and 60% relative humidity of gas fed to cathode. A 2^k factorial design was carried out to explore the effects of various parameters including the flow rate of H_2 (A, 80-200 sccm), flow rate of O_2 (B, 80-200 sccm), cell temperature (C, 39-70 °C) and cell voltage (D, 0.55-0.80 V) on the ohmic resistance (R_{Ω}), the charge transfer resistance (R_{ct}) and the capacitance (C_d).

RESULTS AND DISCUSSION

1. Regression Model and Analysis of Variance (ANOVA)

The application of 2^k factorial design offers an empirical relationship between the response parameters in a fuel cell (ohmic resistance, charge transfer resistance and capacitance) and its operating conditions. The 2^k factorial design was conducted with 2 replications, 3 center points and 6 axial points (Table 1) and the level of confidence of 95%, the critical value of F_0 ($F_{0.05,1,27}$), was 4.21 [22].

According the ANOVA results of ohmic resistance (Table 2), it was found that the F_0 values of A, A^2, B^2, and D^2 were lower than the critical value. This means that the feed rate of oxygen (B), cell temperature (C), cell voltage (D) and interaction of all variables (C^2, AB, AC, AD, BC, BD, ABC, ABD, ACD, BCD, ABCD) had significant effect on the ohmic resistance. The obtained regression model can be expressed in terms of the logarithmic ohmic resistance as written by Eq. (1). The coefficient of determination (R^2) of this equation was obtained at 0.9545 and residual of this equation was found to be distributed randomly. This implies that the regression model was fitted and can be used to represent the data in the experimental range. On the other hand, for charge transfer resistance, all parameters besides feed rate of hydrogen (A) and an interaction between feed rate of oxygen and temperature (BC) have a strong influence on the charge transfer resistance, whereas only temperature (C), cell voltage (D), interaction of hydrogen feed rate and temperature (AC), interaction of feed rate of both gases and temperature (ABC), interaction of feed rate of oxygen, temperature and cell voltage (BCD)

Table 2. ANOVA table

Source	Degree of Freedom	Log R_{Ω} (Ω)			Log R_{ct} (Ω)			Log C_d (μF)		
		Sum of Squares	Mean Square	F-Value	Sum of Squares	Mean Square	F-Value	Sum of Squares	Mean Square	F-Value
A	1	0.0040	0.0040	1.6737	0.0049	0.0049	1.1748	0.0247	0.0247	3.0753
B	1	0.0365	0.0365	15.249	0.0391	0.0391	9.3526	0.0036	0.0036	0.4423
C	1	2.2487	2.2486	939.22	2.5915	2.5915	620.35	2.8179	2.8179	350.25
D	1	0.1692	0.1692	70.673	4.0964	4.0964	980.57	0.9291	0.9291	115.48
A^2	1	0.0002	0.0002	0.0852	0.0384	0.0384	9.1867	0.0051	0.0051	0.6346
B^2	1	0.0004	0.0004	0.1851	0.0337	0.0337	8.0621	0.0285	0.0285	3.5448
C^2	1	0.1335	0.1335	55.765	0.5418	0.5418	129.68	0.2811	0.2811	34.943
D^2	1	0.0027	0.0027	1.1321	0.0794	0.0794	19.012	0.0033	0.0033	0.4142
AB	1	0.0431	0.0431	18.009	0.0329	0.0329	7.8653	0.0267	0.0267	3.3152
AC	1	0.1447	0.1447	60.449	0.1811	0.1811	43.352	0.1660	0.1660	20.630
AD	1	0.0211	0.0211	8.8036	0.0358	0.0358	8.5753	0.0018	0.0018	0.2240
BC	1	0.0465	0.0464	19.399	0.0063	0.0063	1.5069	0.0297	0.0297	3.6875
BD	1	0.0510	0.0510	21.312	0.0194	0.0194	4.6479	0.0129	0.0129	1.6013
CD	1	0.0145	0.0144	6.0487	0.2667	0.2667	63.833	0.0040	0.0040	0.4985
ABC	1	0.0651	0.0651	27.195	0.0180	0.0180	4.3142	0.1088	0.1088	13.522
ABD	1	0.6590	0.6590	275.25	0.5571	0.5571	133.35	0.3301	0.3301	41.028
ACD	1	0.0618	0.0617	25.794	0.0540	0.0540	12.925	0.0278	0.0278	3.4567
BCD	1	0.2345	0.2345	97.948	0.3131	0.3131	74.949	0.0508	0.0508	6.3160
ABCD	1	0.3257	0.3256	136.02	0.1583	0.1583	37.893	0.1932	0.1932	24.009
Error	27	0.0646	0.0023		0.1044	0.0042		0.2011	0.0080	
Total	46	4.6222			9.2067			6.0995		

and interaction of all parameters (ABCD) affected the capacitance of fuel cell. Eqs. (2) and (3), respectively, demonstrate the relationship between the logarithmic charge transfer resistance and logarithmic capacitance. Their R^2 values were 0.9454 and 0.9467, respectively, and their residuals were constant variance. It implies that all regression models were fitted and can be used to describe the data in the experimental range.

$$\log R_{\Omega} = -0.2405 - 0.0302x_B + 0.2651x_C - 0.065x_D - 0.2009x_C^2 + 0.0367x_Ax_B - 0.0673x_Ax_C - 0.0381x_Bx_C + 0.0399x_Bx_D + 0.0451x_Ax_Bx_C + 0.1435x_Ax_Bx_D + 0.0439x_Ax_Cx_D + 0.0856x_Bx_Cx_D + 0.1009x_Ax_Bx_Cx_D \quad (1)$$

$$\log R_{ct} = 0.5295 - 0.0313x_B + 0.28461x_C + 0.3578x_D + 0.0748x_A^2 + 0.0701x_B^2 - 0.4540x_C^2 + 0.1334x_D^2 + 0.0320x_Ax_B - 0.0752x_Ax_C + 0.0335x_Ax_D - 0.0913x_Cx_D + 0.1319x_Ax_Bx_D + 0.0411x_Ax_Cx_D + 0.0989x_Bx_Cx_D + 0.0703x_Ax_Bx_Cx_D \quad (2)$$

$$\log C_d = 4.0002 - 0.2967x_C + 0.1622x_D + 0.3124x_C^2 + 0.0720x_Ax_C - 0.0583x_Ax_Bx_C - 0.1016x_Ax_Bx_D - 0.0398x_Bx_Cx_D - 0.0777x_Ax_Bx_Cx_D \quad (3)$$

Fig. 1 represents the relationship between the experimental data including ohmic resistance (a), charge transfer resistance (b) and capacitance (c) and the model values predicted by using Eq. (1)-(3). It can be seen that all experimental data were fit very well with the data obtained from model equations with R^2 equal to 0.941, 0.961 and 0.980, respectively.

2. Effect of Parameters on the Cell Performance by EIS

2-1. Effect of H_2 Feed Rate

Fig. 2 shows the impedance spectra of the fuel cell performance by using H_2 feed rate of 80 sccm and 200 sccm, which corresponds to a stoichiometric ratio of H_2 to O_2 of 1 : 2 and 1 : 0.8, respectively, under the controlled condition of 80 sccm O_2 feed rate, 0.8 V and 39 °C cell temperature at 60% relative humidity of cathode and saturated humidification at anode. The results exhibited that both impedance arcs at high frequency are obviously similar as they provided approximately 0.21 Ω ohmic resistances. This indicated that the feed rate of H_2 had no effect on the ohmic resistance of the single fuel cell. However, focusing on the total size of both spectra, it can be seen that the impedance spectra at the high H_2 feed rate were a little bit larger than that at low H_2 feed rate. In addition, the imaginary part of the former was also higher than that of the latter, which means that the charge resistance of the fuel cell using high H_2 feed rate was larger than the fuel cell using the low H_2 feed rate. This might be attributed to the effect of water in the feed gas. Namely, by using a higher H_2 feed rate, a large amount of water came to the system. This amount of water may have accumulated on the catalyst surface and barricaded the oxidation reaction, leading to the increase in charge transfer resistance.

2-2. Effect of O_2 Feed Rate

Fig. 3 displays the effect of feed rate of O_2 at 80 sccm and 200 sccm, which corresponds to a stoichiometric ratio of H_2 to H_2 of 1 : 2 and 1 : 5, respectively, under the controlled condition including the cell voltage of 0.8 V, cell temperature of 39 °C, and feed rate of H_2 of 80 sccm. The results revealed that the feed rate of O_2 had very slightly affected the ohmic resistance of the fuel cell, around 0.20-0.21 Ω. However, it had a significant effect on the charge transfer

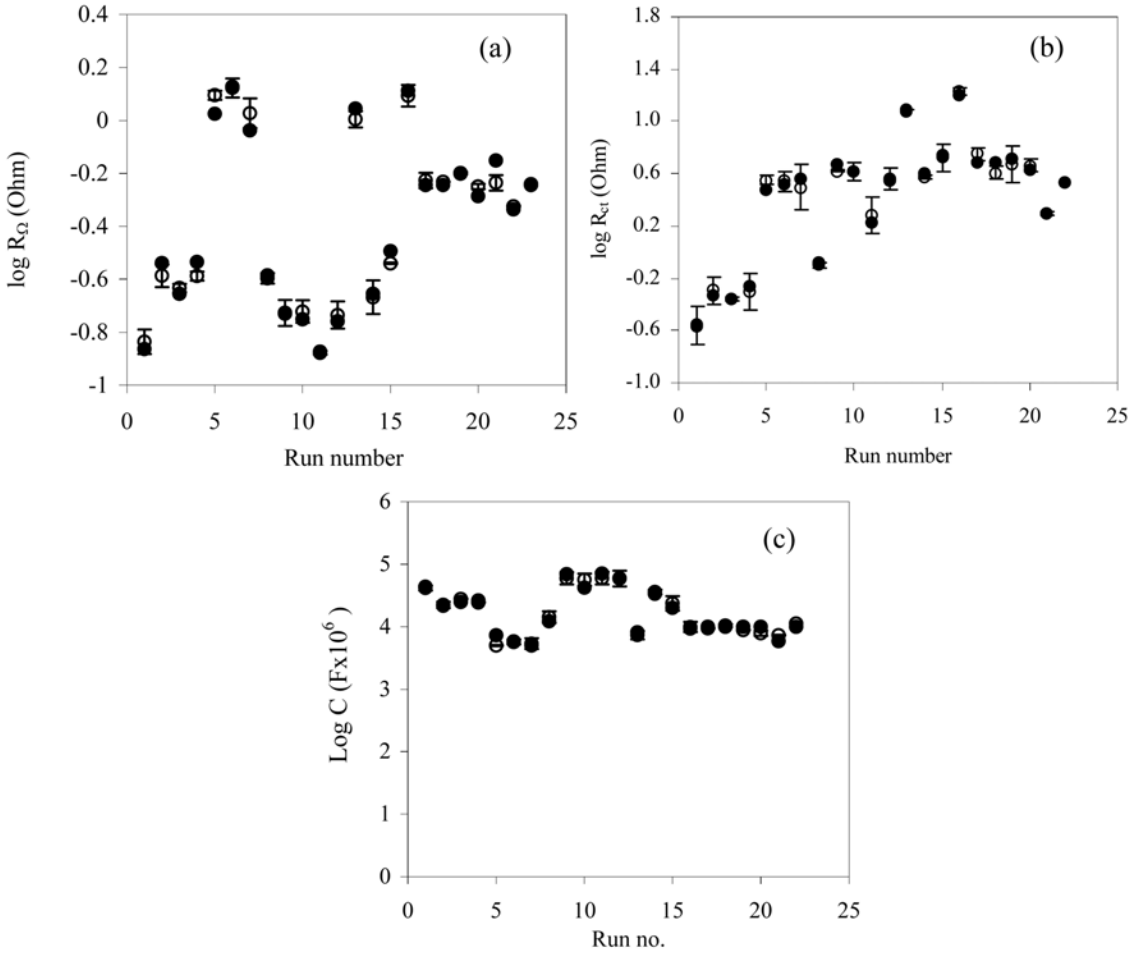

Fig. 1. Comparison plot of the experimental data (○) and predicted values (●) of (a) Eqs. (1); (b) Eq. (2) and (c) Eq. (3).

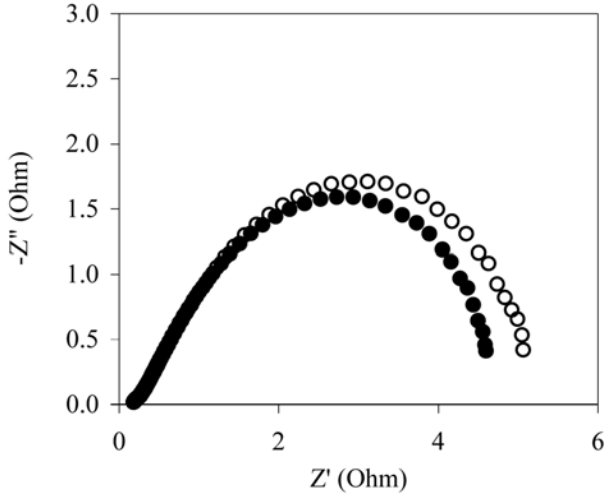

Fig. 2. Nyquist plot of PEM fuel cell performance at H_2 feed rate of 80 sccm (●) and 200 sccm (○), feed rate of O_2 of 80 sccm, cell voltage of 0.8 V and cell temperature of 39 °C.

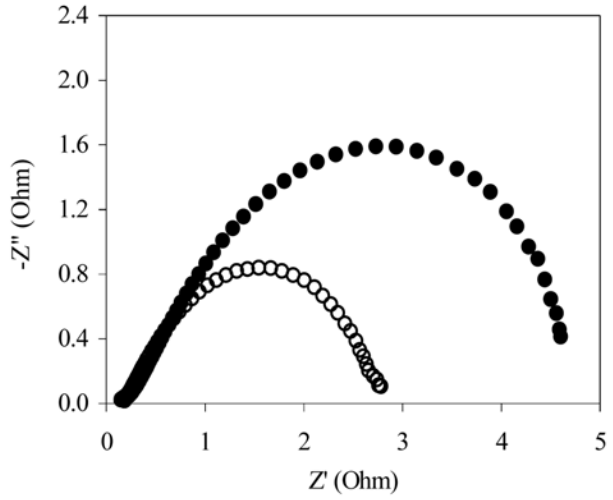

Fig. 3. Nyquist plot of PEM fuel cell performance at O_2 feed rate of 80 sccm (●) and 200 sccm (○), feed rate of H_2 of 80 sccm, cell voltage of 0.8 V and cell temperature of 39 °C.

resistance. Namely, the impedance spectra of fuel cell using the high O_2 feed rate was smaller than that using the low O_2 feed rate of approximately 2 times. There are at least two reasons why the fuel cell performance improves with a higher O_2 feed rate: first, a high feed rate helps to remove the produced water from fuel cell, and second, a higher feed rate keeps a high O_2 concentration leading to a

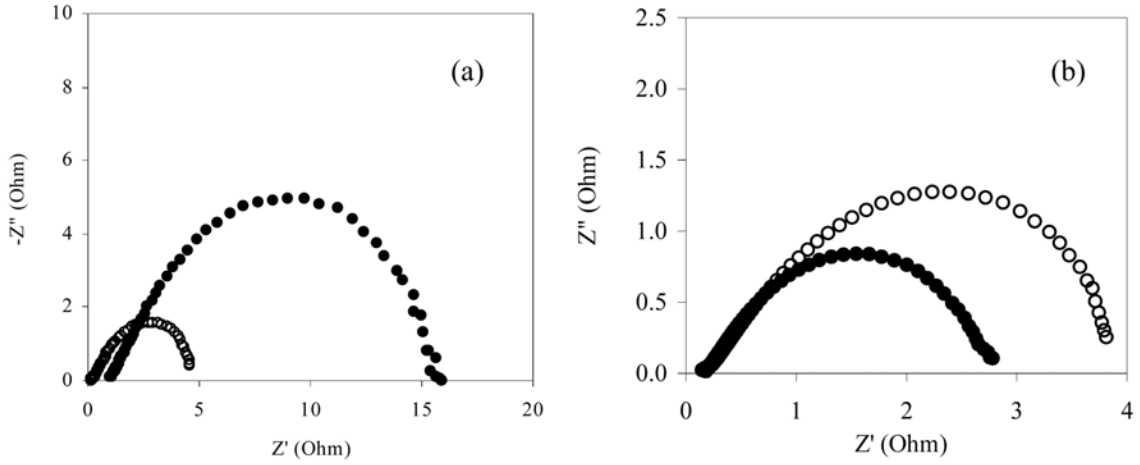

Fig. 4. Nyquist plot of PEM fuel cell performance at cell temperature of 39 °C (○) and 70 °C (●), feed rate of H_2 and O_2 of 80 sccm and cell voltage of 0.8 V with 60% relative humidity (a) and 100 relative humidity at cathode (b).

lower charge transfer resistance and a higher cell performance [23].

2-3. Effect of Cell Temperature and Humidification

The effect of cell temperature was investigated at 39 °C and 70 °C under controlled conditions (equal feed rate of H_2 and O_2 of 80 sccm and cell voltage of 0.8 V). Considering the cell using the 60% relative humidity at cathode (Fig. 4(a)), the impedance spectra at high frequencies of low cell temperature were lower than that at high cell temperature. It indicates that the ohmic resistance of low cell temperature fuel cell was lower than that of high temperature fuel cell. In addition, the charge transfer resistance of the former was lower than that of the latter of approximately 3-fold, which conflicted with the results of Freire and Gonzalez [15]. However, by using 100% relative humidity for both sides (Fig. 4(b)), the ohmic resistance and charge transfer resistance of the higher cell temperature were lower than that at low cell temperature. This behavior may have led to the effect of low relative humidity at cathode; namely, when the high cell temperature was carried out at low relative humidity, the free water contained in the cell evaporating led to the dehydration of membrane leading to the higher ohmic resistance and charge transfer resistance. However, if a high cell temperature was applied at high relative humidity, a similar result with Freire and Gonzalez [15] was obtained. This hypothesis was proved by making the water balance around the single cell at 60% relative humidity at cathode and

Table 3. Water balances a round the single fuel cell at 60% relative humidity in cathode and saturated humidification in anode (Basis 1 min calculation)

Sources of water	Amount of H_2O (mole)
Water inlet with H_2 gas	9.04×10^{-5}
Water outlet from anode	8.72×10^{-5}
Total water in anode (A)	0.32×10^{-5}
Water inlet with O_2 gas	5.89×10^{-5}
Water produced by the reaction in cathode	4.04×10^{-6}
Water outlet from cathode	7.30×10^{-5}
Total water in cathode (B)	-1.006×10^{-5}
Total water in cathode [(A)+(B)]	-0.686×10^{-6}

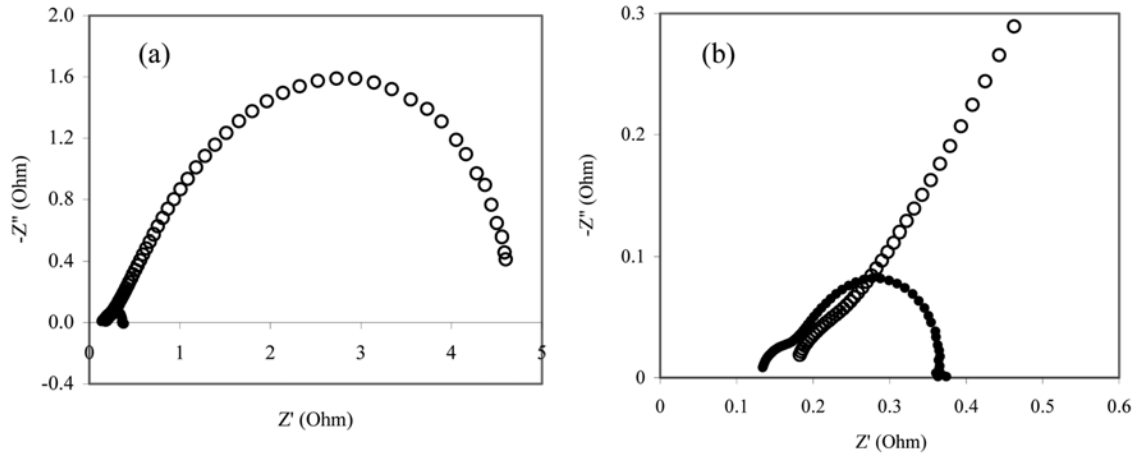

Fig. 5. Nyquist plot of PEM fuel cell performance at cell voltage of 0.55 V (●) and 0.80 V (○) by using equal feed rate of H_2 and O_2 of 80 sccm and cell temperature of 39 °C at all frequencies (a) and high frequency range (b).

Table 4. Operating condition of fuel cell at different respondent parameters at 5th level significant designed by Design-Expert 6.0.10 version

Condition no.	Important response parameters (5th level)	Operating condition of fuel cell			
		Feed rate of H_2 (sccm)	Feed rate of O_2 (sccm)	Temperature (°C)	Cell voltage (V)
1	R_{Ω}-R_{ct}-C_d/R_{Ω}-C_d/R_{ct}-C_d/R_{Ω}/C_d	200	200	70	0.55
2	R_{ct}	118	140	39	0.55
3	R_{Ω}-R_{ct}	94	140	39	0.55

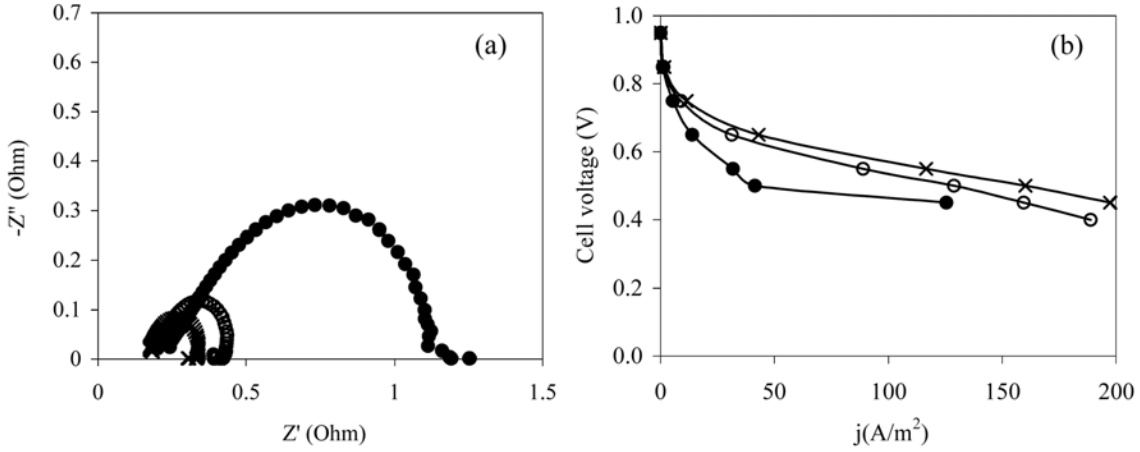

Fig. 6. Nyquist plot (a) and Polarization curve (b) of fuel cell at various conditions of Table 4. Condition 1 (●); Condition 2 (○) and Condition 3 (×).

saturated humidity at anode (Table 3). It showed that approximately 0.32×10^{-5} moles of water occupied the anode, whereas there was no amount of water in the cathode (-1.006×10^{-5} mole). It implied that a lack of water in the cathode occurred and the previous hypothesis concerning that the cell was dried at high temperature at 60% relative humidity was correct.

2-4. Effect of Cell Voltage

Fig. 5 demonstrates the effect of cell voltage at 0.55 V and 0.8 V by using the equal feed rate of H_2 and O_2 of 80 sccm and cell temperature of 39 °C. The results indicated that the impedance spectra at high cell voltage were larger than that at low cell voltage (Fig. 5(a)). This indicates that the charge transfer resistance at high cell voltage was higher than that at low cell voltage. Focusing on the high frequency region of the Nyquist plot in Fig. 5(b), it can be seen that a small second incomplete semi-circle can be detected for both cell voltages. In addition, this second semi-circle was strongly observed at low cell voltage spectra similar to the results of Romero-Castanon et al. [13]. These incomplete semi-circle spectra were the response of the anode side, which are usually smaller than that of cathode side [24]. Also, considering the ohmic resistance at high frequency region, it can be seen that the ohmic resistance of the low cell voltage was a little bit lower than that at high cell voltage. This may have led to the large amount of water produced at low cell voltage (0.55 V) leading to the back diffusion of free water through the membrane. If we take a closer look at the low frequency region of Nyquist plots of the spectra at 0.55 V, it is clearly observed that a fluctuation of the impedance spectra was obtained. This is due to flooding at the cathode side.

3. Determination of Optimum Condition using EIS

Determination of optimum condition using the above empirical relations cannot be performed due to the complication of the developed model equations. Therefore, the optimum operating condition was investigated by using the computer program known as "Design-Expert 6.0.10 version. In the program, the important levels are sorted into 5 levels; the 5th level is the highest importance while the 1st level is the lowest importance. Table 4 demonstrates three conditions that provided the significance of parameters at the 5th level. For example, for the 1st condition, the important parameters were focused on the R_{Ω}-R_{ct}-C_d or R_{Ω}-C_d or R_{ct}-C-$_d$ or R_{Ω} or C_d and the operating conditions were 200 sccm H_2, 200 sccm O_2, 70 °C and 0.55 V.

Fig. 6(a) shows the performance curve of a fuel cell operated at various conditions according to Table 4. It demonstrates that the impedance spectra of the 3rd condition are smaller than that of other conditions. The ohmic resistance, charge transfer resistance and capacitance were 0.1743 Ω, 0.2454 Ω and 31,337 μF, respectively. The results were also confirmed by the polarization curve (Fig. 6(b)). The results agreed very well with the Nyquist plot; namely, the 3rd condition provides the highest cell performance. It gives approximately 239 mA/cm^2 or around 0.40 W at 0.35 V. Comparing the response values predicted by using Eqs. (1)-(3) and the experiment data performed according to conditions of Table 4, it can be seen that all values obtained by using both methods were closely similar with an error less than 10%. This emphasized that the model equation has the reliability to predict all responses including ohmic resistance, charge transfer resistance, and capacitance.

The equivalent circuit of the single fuel cell was also determined by using the FRA program and demonstrated in Fig. 7. It can be seen that the circuit was comprised of two loops with χ^2=1.546. The left-hand side loop is concerned with the properties of the anode,

Table 5. Response values predicted by using Eqs. (1)-(3) and by experiment according to condition of Table 4

Condition no.	Response								
	R_Ω (Ω)			R_{ct} (Ω)			C_d (μF)		
	Experiment	Eq. (1)	Error* (%)	Experiment	Eq. (2)	Error (%)	Experiment	Eq. (3)	Error (%)
1	0.2409	0.2608	8.26	0.7789	0.8374	7.51	11,523	12,191	5.80
2	0.1992	0.2127	6.78	0.3369	0.306	9.17	26,640	28,293	6.20
3	0.1743	0.1862	6.83	0.2454	0.2664	8.56	31,337	31,622	0.91

$$*\text{Error}\ (\%) = \left(\frac{\text{experimental value} - \text{predicted value from model equations}}{\text{experimental value}}\right) \times 100$$

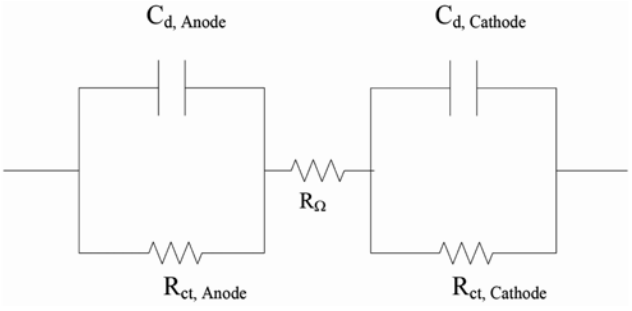

Fig. 7. Equivalent circuit.

Table 6. Composition of equivalent circuit

Equivalent circuit elements	Value	χ^2
R_Ω	0.170	1.546
R_{ct}, anode (Ω)	0.023	
R_{ct}, cathode (Ω)	0.157	
C_d, anode (F)	0.021	
C_d, cathode (F)	0.165	

and the right-hand side loop reveals the properties of the cathode. Table 6 shows the value of ohmic resistance, charge transfer resistance and capacitance of the equivalent circuit. Both resistances observed in cathode were greater than that in anode by approximately 6-7-fold.

CONCLUSION

This work aims to investigate the influence of several parameters on the performance of PEMFC by using electrochemical impedance spectroscopy (EIS) together with the 2^k factorial design. The preliminary results indicated that the cell temperature, the cell voltage and the interaction of cell voltage, flow rates of H_2 and O_2 had significant effects on the cell performance. In addition, the flow rate of O_2 had a strong effect on the ohmic resistance (R_Ω) and charge transfer resistance (R_{ct}) in the system. The good relationship between the model equations and experimental data were obtained with the coefficient of determination greater than 0.94. The optimum operating condition was also determined by using the Design-Expert 6.0.10 version. It demonstrated that the maximum cell performance was obtained by focusing the $R_\Omega R_{ct}$ as the important parameters and the predicted response values deviated from the experimental data were less than 10%.

ACKNOWLEDGMENTS

The authors would like to thank the ADB under The Petroleum and Petrochemical Technology Consortium, Chulalongkorn University and The National Metal and Materials Technology Center (MTEC) for financial support of our project.

REFERENCES

1. H. Shinichi, K. Jumbom and S. Supramaniam, *Electrochimica Acta*, **42** (10), 1587 (1997).
2. M. Bron, P. Bogdanoff, S. Fiechter, M. Hilgendorff, J. Radnik, I. Dorbandt, H. Schulenburg and H. Tributsh, *J. Electroanal. Chem.*, **517**(2), 85 (2001).
3. W. Hawut, M. Hunsom and K. Pruksathorn, *Korean J. Chem. Eng.*, **23**, 555 (2006).
4. V. A. Paganin, C. L. F. Oliveira, E. A. Ticianelli, T. E. Springer and E. R. Gonzalez, *Electrochim. Acta.*, **43**, 3761 (1998).
5. H. Mali, L. A. Dunyushkina and S. B. Adler, *Korean J. Chem. Eng.*, **23**, 720 (2006).
6. M. J. Jorgensen, P. Primdahl and M. Mogensen, *Electrochimica Acta*, **44**, 4195 (1999).
7. H. K., Lee, *Mat. Chem. Phys.*, **77**, 639 (2002).
8. C. M. Lai, J. C. Lin, K. L. Hsueh, C. P. Hwang, K. C. Tsay, L. Tsai and Y. M. Peng, *Int. J. Hydrogen Energ.*, Article in Press.
9. C. Y. Du, T. S. Zhao and C. Xu, *J. Power Sources*, **167**(2), 265 (2007).
10. C. Y. Du, T. S. Zhao and W. W. Yang, *Electrochimica Acta*, **52**(16), 5266 (2007).
11. N. Wagner, W. Schnurnberger, B. Muller and M. Lang, *Electrochim. Acta.*, **43**(24), 3785 (1998).
12. M. Eikerling and A. A. Kornyshev, *J. Electroanal. Chem.*, **475**, 107 (1999).
13. T. Romero-Castañón, L. G. Arriaga and U. Cano-Castillo, *J. Power Sources*, **118**(1-2), 179 (2003).
14. E. B. Easton, P. G. Pickup, *Electrochim. Acta.*, **50**, 2469 (2005).
15. T. J. P. Freire and E. R. Gonzalez, *J. Electroanal. Chem.*, **503**, 57 (2000).
16. B. Andreaus, A. J. McEvoy and G. G. Scherer, *Electrochim. Acta.*, **47**(13-14), 2223 (2002).
17. M. Ciureanu and R. Roberge, *J. Phy. Chem. B*, **105**(17), 3531 (2001).
18. T. E. Springer, T. A. Zawodzinski, M. S. Wilson and S. Gottesfeld, *J. Electrochem. Soc.*, **143**(2), 587 (1996).

19. N. Wagner and M. Schulze, *Electrochim. Acta*., **48**, 3899 (2003).
20. C. A. Schiller, F. Richter, E. Gulzow and N. Wagner, *Phys. Chem. Phys*., **3**, 2113 (2001).
21. D. Yang, J. Ma, L. Xu, M. Wu and H. Wang, *Electrochim. Acta*., **51**, 4039 (2006).
22. D. C. Montgomery, *Design and analysis of experiments*, 5th ed. John Wiley & Sons Ltd., New York (2001).
23. F. Barbie, *PEM fuel cells, Theory and practice*, Elsevier Academic Press, USA (2005).
24. R. O'Hayre, S. W. Cha and W. Colella, *Fuel cell fundamentals*, John Wiley & Sons, New York (2006).